Eur. Phys. J. D **12**, 435–448 (2000)

THE EUROPEAN PHYSICAL JOURNAL D

EDP Sciences

A theoretical study of CO_2 and N_2O molecules trapped in an argon matrix: Vibrational energies, and transition moments for low-lying levels and IR bar spectra

A. Lakhlifi[1,a], H. Chabbi[2], P.R. Dahoo[2,b], and J.L. Teffo[2]

[1] Laboratoire d'Astrophysique de l'Observatoire de Besançon[c], 41 bis avenue de l'Observatoire, B.P. 1615, Université de Franche-Comté, 25010 Besançon Cedex, France
[2] Laboratoire de Physique Moléculaire et Applications[d], Université P. et M. Curie, Tour 13, Boîte 76, 4 place Jussieu, 75252 Paris Cedex 05, France

Received 22 March 2000 and Received in final form 10 May 2000

Abstract. Semi-empirical atom-atom potential energy calculations based on pairwise additive interactions are performed and, after applying the Born-Oppenheimer approximation to separate high frequency vibrational modes from low frequency orientational and translational modes, the infrared vibrational spectra of CO_2 and N_2O monomers trapped in an argon matrix at a temperature of 5 K are determined. It is shown that only a double substitutional site in argon can accommodate N_2O, whereas CO_2 is trapped in two distinct sites, of single and double substitutional types. The model shows that splitting of the degenerate ν_2 mode occurs for both molecules in the double site. In the ground electronic state, the vibrational frequency shifts due to the matrix and the vibrational transition moments for low-lying levels are determined using the contact transformation method, as used for gas phase calculations. Calculated energy levels compare well with observed ones and the theory also predicts some unobserved levels. Moreover, calculations show no significant changes in the dipole moments of both CO_2 and N_2O trapped molecules.

PACS. 33.20.-t Molecular spectra – 33.20.Ea Infrared spectra

1 Introduction

In an argon matrix, carbon dioxide is known to be trapped in two different trapping sites, one termed stable and the other unstable, because it disappears after strong annealing. By taking into account the facts that both sites are stable if annealing of the argon matrix is mild and that below 25 K the temperature effect on line widths and shifts is negligible, the nature of the two trapping sites was determined in reference [1]. At the harmonic level of approximation, a splitting of the doubly degenerate ν_2 bending mode was shown to occur in the double distorted substitutional site (assigned to be the unstable site because of its asymmetry).

In the theoretical model described in reference [1], the fundamental frequencies (ω_2 and ω_3) calculated at the harmonic level are adjusted to match the observed ones by distorting the matrix atoms around the trapped molecule. The model has been improved and applied to the non-linear triatomic molecule O_3 trapped in rare gas matrices [2,3]. Vibrational frequencies are calculated by contact transformation perturbation methods and adjusted to those observed in the spectral region below 4 000 cm^{-1}. The formulae given by Nielsen [4] and Flaud *et al.* [5] for the calculation of the vibrational energies, can be applied straightforwardly to take into account the effects of Coriolis and Darling-Dennison resonances.

In this work, the improved model is applied to two linear triatomic molecules CO_2 and N_2O. In the latter case, it has been observed that the molecule is trapped in only one site in argon [6,7], with a splitting of the ν_2 degenerate mode, as for CO_2 in its unstable site. Sodeau *et al.* [6] suggest a double substitutional trapping site to explain this splitting for N_2O. In free standing crystals of argon, Apkarian *et al.* [8] show that, contrary to its behaviour under matrix isolation techniques, N_2O tends to form dimers. The vibrational energies of the monomers are then shifted by a different amount.

[a] e-mail: azzedine.lakhlifi@iut-bm.univ-fcomte.fr
or e-mail: azzedine.lakhlifi@obs-besancon.fr
Also at: Département d'Organisation et Génie de la Production, Institut Universitaire de Technologie de Belfort-Montbéliard, France.
[b] e-mail: prd@carnot.physique.uvsq.fr
Is now at Laboratoire de Magnétisme et d'Optique de l'Université de Versailles, 45 avenue des États-Unis, 78035 Versailles Cedex, France.
[c] UPRES A CNRS 6091
[d] UPR CNRS 136

The aim of the present work is to determine the nature of the trapping site for N_2O in argon, as was done for CO_2 in reference [1], and to calculate the vibrational energies and transition moments of low-lying levels for both molecules. The results are then compared with recent experimental spectra obtained by using the laser induced fluorescence technique on these systems [9,10]. The free standing crystal case has not been considered. Contrary to the case of O_3, the formulae given by Nielsen and Amat *et al.* [11,12] for linear triatomic molecules cannot be directly used to calculate vibrational energies when a splitting of the ν_2 degenerate mode occurs. A new method treating these two frequencies as quasi-degenerate modes has to be applied, as described in reference [1].

In Section 2, the main steps involved in the determination of the trapping sites are briefly recalled and the separation of the molecular Hamiltonian in the matrix is described. The models applied to solve the vibrational and orientational motions are given in detail and the integrated absorption coefficients are presented. Results are given in Section 3 and a comparison with experiment and discussion are carried out in Section 4.

2 Theory

2.1 The molecular Hamiltonian in the matrix

Rovibrational energy levels of a molecule like CO_2 or N_2O in the gas phase are calculated within the Born-Oppenheimer (BO) approximation in a reference frame satisfying the Eckart-Sayvetz conditions. One then considers the nuclei to be moving in a mean force field which is the gradient of a potential whose minimum corresponds to the stable equilibrium configuration of the nuclei. The Eckart-Sayvetz conditions, which are related to the choice of the reference frame in which the rovibrational degrees of freedom are studied, make it possible to study the latter without considering the translational motion of the molecule.

When the molecule is trapped in a rare gas matrix, it generally replaces one or two atoms in a single or double substitutional site, as shown in Figure 1. Inside such a trapping site, the molecule is no longer free to move as in the gas phase. For small molecules, the frequencies (ω_Q) related to the external degrees of freedom, that is translational and orientational (rotational in the gas phase) motions of the molecule and lattice vibrations of the solid matrix, are smaller than those (ω_q) corresponding to the internal vibrational degrees of freedom. Following the method proposed by Lin [13], a second Born-Oppenheimer (BO) approximation (when $\omega_Q/\omega_q < 0.1$) can thus be applied to study separately the high and low frequency modes. Considering the size of the trapped molecule, compared to that of a substitutional site (single or double in a face-centered-cubic (fcc) or hexagonal-close-packed (hcp) lattice), it is necessary to take into account the distortion of the matrix around the trapped molecule. This distortion, if reasonably small, can be determined by

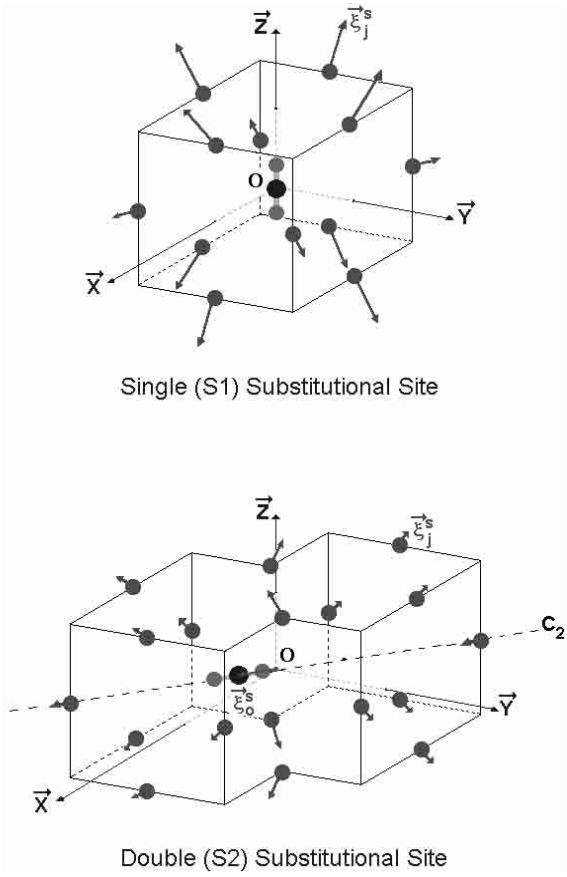

Fig. 1. Definition of the S1 and S2 trapping sites in the face-centered-cubic crystal of an argon matrix. (**X, Y, Z**) defines the absolute frame and arrows characterize the static displacements of the centre of mass of the trapped molecule and the matrix atoms.

the use of the Green tensor of the perfect crystal as applied in the theory elaborated by Flinn and Maradudin [14] to study impurities in perfect crystals. The method "freezes" the external degrees of freedom in a configuration calculated by minimizing the internal energy of the trapped molecule-matrix system at 0 K. One can then determine the configuration for which the free energy of the system is close to its minimum value by adjusting the distortion of the matrix atoms around the trapped molecule (see Fig. 1), as described below in the subsection on the vibrational motion.

In the approximation of a rigid distorted crystal, as determined by the method of Flinn and Maradudin [14], the Hamiltonian H_{M} of a trapped linear molecule in its ground electronic state and its equilibrium position is written as

$$H_{\mathrm{M}} = \sum_i \frac{P_i^2}{2\mu_i} + V_{\mathrm{vib}}(\{q\}) + T_{\mathrm{R}} + V_{\mathrm{M}}^{(n)}(\mathbf{\Omega}, \{q\}). \quad (1)$$

In this equation the first two terms represent the vibrational Hamiltonian of the molecule in the gas phase. In the first term μ_i and $\mathbf{P}_i$ are the reduced mass and the conjugated momentum operator connected to the ith vibrational mode with normal coordinate q_i and frequency

Table 1. Data used in our calculations. Pure Lennard-Jones 12-6 potential parameters (see Eqs. (2, 3) of Ref. [1]), isotropic polarisability of argon atoms and their interdistance in the matrix, and also internal distances, dipole and quadrupole moments and rotational constants of the rigid linear CO_2 and N_2O molecules.

atoms	Ar	C	O	N	internal	CO_2		N_2O	
					characteristics	C–O	N–N		N–O
ϵ^{a} (cm^{-1})	84.0	29.8	39.9	26.5	q_M^e (Å)	1.162	1.128		1.184
σ^{a} (Å)	3.448	3.210	2.882	3.385	${\mu_M^e}^{c}$ (D)	0		0.166	
a^{b} (Å)	3.755	-	-	-	${\Theta_M^e}^{c}$ (DÅ)	–4.3		–3.0	
α^{b} ($Å^3$)	1.639	-	-	-	B_e (cm^{-1})	0.39		0.42	

[a] From reference [28] and references therein. [b] From reference [29]. [c] From reference [30].

ω_i. The second term $V_{\rm vib}(\{q\})$ is the intramolecular potential function, which is generally given as a Taylor series expansion with respect to the dimensionless normal coordinates q. It can be separated into a harmonic part (second order) and an anharmonic one (higher orders), which is considered as a perturbation

$$V_{\rm vib}(\{q\}) = V_{\rm vib}^{\rm har}(\{q\}) + \Delta V_{\rm vib}^{\rm anh}(\{q\}). \qquad (2)$$

The vibrational energies of the molecule in the gas phase are calculated by applying the contact transformation to the anharmonic part of $V_{\rm vib}(\{q\})$ in a perturbation method, as set out in reference [1].

In equation (1), $T_{\rm R}$ is the rotational kinetic Hamiltonian for a rigid linear molecule in the gas phase with rotational constant $B_{\rm e}$. It can be written as

$$T_{\rm R} = -B_{\rm e}\left\{\frac{\partial^2}{\partial\theta^2} + \text{cotan}\,\theta\frac{\partial}{\partial\theta} + \frac{1}{\sin^2\theta}\frac{\partial^2}{\partial\varphi^2}\right\}, \qquad (3)$$

to describe the rotational motion of the molecule in terms of Euler angles $\mathbf{\Omega} = (\varphi, \theta)$ which define the molecular frame (**x**, **y**, **z**) (**z**-axis being the inter-nuclear axis of the molecule) with respect to a crystal absolute frame (**X**, **Y**, **Z**) [1].

The last term $V_{\rm M}^{(n)}(\mathbf{\Omega}, \{q\})$ corresponds to the interaction potential energy experienced by the molecule in the trapping site n with the matrix atoms and the centre of mass of the molecule fixed at the configuration that minimizes the free energy of the molecule-matrix system, as described in reference [1]. In Table 1 we give the potential parameters and characteristics associated with the studied molecule-matrix systems and used in these calculations.

The analysis of the potential energy surfaces shows that $V_{\rm M}^{(n)}(\mathbf{\Omega}, \{q\})$ can be written as the sum of four parts

$$V_{\rm M}^{(n)}(\mathbf{\Omega}, \{q\}) = V_{\rm M}^{(n)\rm e} + V_{\rm M}^{(n)}(\mathbf{\Omega}) + V_{\rm M}^{(n)}(\{q\}) + \Delta V_{\rm M}^{(n)}(\mathbf{\Omega}, \{q\}), \qquad (4)$$

where $V_{\rm M}^{(n)\rm e}$ is the minimum energy value, calculated for the rigid molecule at its equilibrium orientation. The second and third parts respectively describe the angular dependence for the rigid molecule and the vibrational coordinate dependence at the equilibrium orientation. These two terms will be introduced below to renormalise the vibrational and rotational Hamiltonians of the molecule in the gas phase. The last term defines the small dynamical vibration-orientation coupling, which would give rise to a slow population relaxation from the vibrational modes of the molecule into the orientational modes. This term will not be developed in the following sections, since we concentrate on calculating the vibrational frequency shifts and the bar spectrum of the trapped molecule.

2.2 Vibrational motions

In the second BO approximation, one can focus on the vibrational degrees of freedom of the trapped molecule only. The vibrational part of the molecular Hamiltonian is then given by

$$H_{\rm M}^{\rm vib} = \frac{1}{2}\sum_i \omega_i p_i^2 + V_{\rm vib}(\{q\}) + V_{\rm M}^{(n)}(\{q\}), \qquad (5)$$

in which q are now dimensionless normal coordinates (defined in Eq. (10) of Ref. [1]) and p their conjugate momenta.

Since experiments show the vibrational shifts to be small, $V_{\rm M}^{(n)}(\{q\})$ is expanded up to the second order only, in the form

$$V_{\rm M}^{(n)}(\{q\}) = \sum_i \beta_i q_i + \sum_i \sum_{j\geq i} \beta_{ij} q_i q_j, \qquad (6)$$

where β_i and β_{ij} are the first and second derivatives of $V_{\rm M}^{(n)}(\{q\})$ with respect to the dimensionless normal coordinates; their values depend on the trapping site n. Two different electric fields, a static one and a dynamic one, contribute to the latter parameters. The static field is well-known and results from the distortion of the ideal lattice and from the polarization of the matrix atoms by the permanent electric multipoles (dipole and quadrupole moments in the case of N_2O and quadrupole moment in the case of CO_2) of the trapped molecule. Application of the second BO approximation makes it possible to take into account the polarization of the matrix atoms by the dynamical electric field due to the vibrating molecule. In the case of CO_2 and N_2O, this field depends on the derivatives of the dipole moment of the molecule with respect to the dimensionless normal coordinates. Thus the nuclei, because of the effect of the matrix, are moving in a mean

force field (the gradient of a perturbed potential) which is given by

$$U(\{q\}) = \frac{1}{2}\sum_i \omega_i q_i^2 + \Delta V_{\rm vib}^{\rm anh}(\{q\}) + \sum_i \beta_i q_i + \sum_i \sum_{j\geq i} \beta_{ij} q_i q_j, \quad (7)$$

and has a minimum corresponding to a new stable equilibrium configuration of the nuclei. Defining the origin of $U(\{q\})$ at this minimum, and applying an orthogonal transformation to the transformed Hamiltonian in order to eliminate cross terms β_{ij} $(i \neq j)$, the Hamiltonian of the trapped molecule in its ground electronic state and the new equilibrium position of the vibrating nuclei are written as

$$\begin{aligned} H_{\rm M}^{\rm vib} &= H_0' + H_a', \\ H_0' &= \frac{1}{2}\sum_i \omega_i'(p_i'^2 + q_i'^2), \\ H_a' &= \sum_{ijk} k_{ijk}' q_i' q_j' q_k' + \sum_{ijkl} k_{ijkl}' q_i' q_j' q_k' q_l' + \ldots \end{aligned} \quad (8)$$

We have to determine the Hamiltonian which corresponds to a configuration of minimum *internal* energy of the doped matrix. This can be done by numerical simulation using, for example, a Monte Carlo algorithm. This method has not been implemented in the model. Instead, we adjust the static *external* degrees of freedom ($\mathbf{\Omega}$ and $\{Q\}$) to tend to the minimum of the full free energy of the molecule-matrix system. The process is iterative and is halted when the calculated shift of the harmonic frequencies ($\Delta\omega_i^{\rm cal} = \omega_i^{\rm cal}({\rm matrix}) - \omega_i^{\rm cal}({\rm gas})$) fits the experimentally observed fundamental shift ($\Delta\omega_i^{\rm obs} = \omega_i^{\rm obs}({\rm matrix}) - \omega_i^{\rm obs}({\rm gas})$).

The distortion is thus determined by taking advantage of the fact that the shifts of the vibrational levels of the embedded molecule in its ground electronic state depend on the electric field at the trapping site. Moreover, as this field is due to the surrounding matrix atoms modified by their distortion and their polarization by the non-zero electric multipolar moments of the embedded molecule, the method is partly self-consistent. This is due to the fact that the polarization of the matrix atoms is a function of two parameters, the molecular dynamical electric moment and the distortion of the trapping site, while the former parameter is also a function of the latter one. The calculated shift is achieved by an iterative procedure previously described in Section 2 of reference [1].

Perturbation theory can then be applied to H_a', using the wave functions of H_0' as a zeroth order basis, following the method described in reference [1]. For molecules trapped in a double substitutional site, the splitting of the ν_2 mode means that a degenerate perturbation theory using the three dimensional Wang basis [15] has to be applied [1].

One may note that these levels can be determined from observed values, as was done in references [16–18] for O_3, from a calculation of force constants on the basis of a general harmonic force field. This implies, of course, that a sufficient number of observed values are available for all the isotopic species to give a reliable fit. The method which we are adopting instead relies on good *ab initio* parameters. It is clear that since atom-atom potentials are effective pair potentials, their parameters contain contributions from many-body interactions [19]. By the use of such parameters we assume implicitly that the trapped molecule preserves its individual properties and that no complexes of any kind, such as a charge transfer complex for instance, are being formed.

2.3 Angular motions

The orientational Hamiltonian of the rigid molecule trapped in the matrix is the sum of the rotational kinetic operator $T_{\rm R}$ defined in equation (3) and the orientational potential part $V_{\rm M}^{(n)}(\mathbf{\Omega})$ of equation (4) which strongly depends on the trapping site.

Analysis of the angular potential surfaces $V_{\rm M}^{(n)}(\mathbf{\Omega})$ shows that the **z** molecular axis can exhibit either a one-dimensional librational motion around the orientational equilibrium position $\theta^{\rm e} = 0$, with φ corresponding to free motion, or two-dimensional librational motion around $\theta^{\rm e} = \pi/2$ and $\varphi^{\rm e}$ ($\varphi^{\rm e} = 0$ or $\varphi^{\rm e} = \pi/2$). The angular variables θ in the first case and θ and φ in the second one are not appropriate for defining good librational quantum numbers. They can be replaced by the new variables $u_\theta = \tan(\theta/2)$ and $u_\theta = \cos\theta$ and $u_\varphi = \varphi - \varphi^{\rm e}$, respectively, which characterize small angular oscillations of the **z** molecular axis. $V_{\rm M}^{(n)}(\mathbf{\Omega})$ can then be expanded as a power series in the new variables, in which the harmonic terms are much greater than the anharmonic ones.

Thus, using the harmonic oscillator bases, the eigensolutions of the orientational Hamiltonian are given by

$$\begin{aligned} E_{jM}^{(n)} &= \hbar\omega_\theta\,(2j - |M| + 1) \ \text{ in which } \hbar\omega_\theta = 2\alpha_\theta B_{\rm e}, \\ |jM\rangle^{(n)} &= N_j^{|M|} \exp(-u_\theta^2/2) u_\theta^{|M|} L_j^{|M|}(u_\theta^2) \exp[{\rm i}(M\varphi)], \end{aligned} \quad (9)$$

for the first case, and

$$\begin{aligned} E_{jm}^{(n)} &= \hbar\omega_\theta(j + 1/2) + \hbar\omega_\varphi\,(m + 1/2)\,, \\ |jm\rangle^{(n)} &= N_j N_m \exp[-(u_\theta^2 + u_\varphi^2)/2] H_j(u_\theta) H_m(u_\varphi), \end{aligned} \quad (10)$$

for the second one.

In equations (9) the parameter α_θ is proportional to the square root of the harmonic coefficient of the $V_{\rm M}^{(n)}(\mathbf{\Omega})$ expansion, N is a normalization factor, and L are the associated Laguerre functions. The librational quantum number j is an integer number and the free rotational quantum number M obeys the condition $|M| \leq j$. In equations (10) ω, N and H are the librational harmonic frequencies, the normalization factors and the Hermite polynomials, connected to the two librational motions, respectively. Note

that the quantum numbers j and m are independent integer numbers.

Finally when the remaining terms of the orientational Hamiltonians are introduced as perturbations, the eigenenergies become $\mathcal{E}_{jM}^{(n)}$ and $\mathcal{E}_{jm}^{(n)}$, respectively. Note however that the ratios $|\mathcal{E}-E|/E$ do not exceed ~ 0.1 for the lowest energy levels.

2.4 Absorption coefficient

The absorption coefficient for $\mathcal{N}$ trapped molecules (monomers) per volume unit is defined as a function of the frequency position ω by

$$I(\omega) = \frac{4\pi\omega\mathcal{N}}{3hc}\mathrm{Re}\int_0^\infty \mathrm{d}t\,\mathrm{e}^{-\mathrm{i}\omega t}\mathrm{Tr}\left[\boldsymbol{\mu}_A(0)\boldsymbol{\mu}_A(t)\rho(0)\right], \quad (11)$$

where c is the vacuum light velocity, $\rho(0)$ characterizes the initial canonical density matrix associated with the total system, and $\boldsymbol{\mu}_A$ is the molecular dipole moment expressed in the crystal absolute frame (see Appendix A). The Re symbol defines the real part of the Fourier transform of the trace (Tr) operation over the time evolution of this system.

As has been mentioned above, in this work we are interested in calculating the infrared bar spectra of the CO_2 and N_2O linear molecules trapped in argon matrices. However, some assumptions and conditions have been necessary in order to perform the calculations.

(i) Since experiments are performed with highly diluted samples, our calculations used 1060 atoms to simulate the argon matrix. The mutual interactions between trapped molecules are then negligible.

(ii) The radiation processes for each molecule occur in a distorted and static cage *i.e.* the matrix atoms are fixed at their equilibrium positions which minimize the *internal* energy of the doped matrix. The dynamical coupling between the optical (vibration and orientation) modes and the bath (lattice and molecular c.m. translations) modes is then ignored.

(iii) The initial chaos hypothesis is assumed to be valid and this allows us to write the optical state $|...v...jm\rangle^{(n)}$ as the product of the renormalized vibrational and orientational states $|...v...\rangle \times |jm\rangle^{(n)}$ in which m designates M of equations (9) or m of equations (10) according to whether the molecule moves orientationally around $\theta^{\mathrm{e}} = 0$ or $\theta^{\mathrm{e}} = \pi/2$ positions, respectively.

(iv) As we will see in the following section, when two trapping sites are possible, the number $\mathcal{N}$ defined in equation (11) is the sum $\mathcal{N}^{(1)} + \mathcal{N}^{(2)}$ of the numbers of trapped monomers per volume unit in the single ($n = 1$) and double ($n = 2$) substitutional sites, respectively.

(v) Finally, when the molecules are trapped in the single site, there are three possible orientational equilibrium positions (along **X**, **Y** or **Z**-axes). Then, one can suppose that these three orientations are statistically equiprobable.

Within these approximations, the absorption coefficient of the trapped molecules in the site n and connected to the kth vibrational fundamental transitions $|...0_k...\rangle|j_i m_i\rangle^{(n)} \rightarrow |...1_k...\rangle|j_f m_f\rangle^{(n)}$ with energies $\mathcal{E}_{0_k j_i m_i}^{(n)}$ and $\mathcal{E}_{1_k j_f m_f}^{(n)}$ and frequency shift $\Delta\omega_k^{(n)}$ is written as

$$\begin{aligned} I_k^{(n)}(\omega) = {} & \frac{8\pi^2}{3hc}\omega\mathcal{N}^{(n)}\left|\langle...0_k...|q_k|...1_k...\rangle\right|^2 \\ & \times \sum_{j_i m_i j_f m_f} \frac{\mathrm{e}^{-\beta\mathcal{E}_{0_k j_i m_i}^{(n)}} - \mathrm{e}^{-\beta\mathcal{E}_{1_k j_f m_f}^{(n)}}}{Z^{(n)}} \\ & \times \left|\left\langle j_i m_i \left|\frac{\partial\boldsymbol{\mu}_A}{\partial q_k}\right| j_f m_f\right\rangle^{(n)}\right|^2 \\ & \times \delta\left(\omega - \Delta\omega_k^{(n)} - \hbar^{-1}\left(\mathcal{E}_{1_k j_f m_f}^{(n)} - \mathcal{E}_{0_k j_i m_i}^{(n)}\right)\right). \end{aligned} \quad (12)$$

In this equation the $\langle...\rangle$ brackets represent the transition elements of the dimensionless normal coordinate q_k connected to the kth vibrational mode on one hand, and of the first derivative of the molecular dipole moment with respect to this coordinate (see Appendix A) on the other hand. The indices i and f characterize the initial and final orientational states in the transition, Z defines the vibration-orientation canonical partition function at temperature T, $\beta = (k_{\mathrm{B}}T)^{-1}$, and δ is the Dirac function.

3 Results

3.1 Equilibrium configurations

The application of the theoretical model described in reference [1] led to the equilibrium characteristics that have been given previously for the CO_2 molecule. The model applied in this work leads to very slightly different results. We recall that the CO_2 molecule can be trapped in two different sites. In the single substitutional site termed S1, the centre of mass of the molecule is located at the site centre with its **z**-axis parallel to one of the C_4 symmetry axes (in the perfect lattice) which coincide with the **X**, **Y** and **Z**-axes of the absolute frame (see Fig. 1). Then the resulting equilibrium orientations are $\theta^{\mathrm{e}} = \pi/2$, $\varphi^{\mathrm{e}} = 0$ and $\pi/2$ for the molecule directed along the **X** and **Y**-axes, respectively, and $\theta^{\mathrm{e}} = 0$ for the molecule directed along the **Z**-axis. The distortion of the argon atoms around the molecule is about 5% of the site diameter for the 8 atoms pertaining to the two perpendicular planes containing the molecular axis, and less than 1% for the 4 atoms in the plane perpendicular to the molecular axis. The corresponding minimum energy value $V_{\mathrm{M}}^{(1)\mathrm{e}}$ is –2 075 cm^{-1}.

In the double substitutional site termed S2, the centre of mass of the molecule is at 0.92 Å on either side

Table 2. Quadratic, cubic and quartic potential constants (cm^{-1}) for dimensionless normal coordinates, for $^{12}CO_2$, $^{13}CO_2$ and $^{14}N_2O$ molecules trapped in the S1 and S2 sites of argon matrices and their values in the gas phase [20,21].

	$^{12}CO_2$			$^{13}CO_2$			$^{14}N_2O$	
	S1	S2	gas	S1	S2	gas	S2	gas
k_{11}	680.49	677.30	676.98	680.16	677.28	676.98	649.18	650.22
k_{2a2a}	333.74	334.71	336.58	324.17	325.05	326.98	298.59	298.25
k_{2b2b}	333.74	334.50	336.58	324.17	324.84	326.98	298.13	298.25
k_{33}	1196.27	1193.24	1198.14	1162.05	1159.01	1164.05	1138.37	1140.79
k_{111}	–45.71	–45.57	–45.56	–45.69	–45.57	–45.56	–59.92	–59.72
k_{113}		0.27			0.34		81.51	80.76
k_{12a2a}	74.87	74.49	74.47	72.70	72.38	72.36	54.20	54.40
k_{12b2b}	74.87	74.49	74.47	72.70	72.38	72.36	54.20	54.40
k_{133}	–249.67	–248.96	–248.93	–242.50	–241.87	–241.84	–225.48	–226.60
k_{2a2a3}		0.15			0.18		51.26	51.06
k_{2b2b3}		0.15			0.18		51.26	51.06
k_{333}		–0.27			–0.33		–65.49	–64.82
k_{1111}	1.87	1.87	1.87	1.87	1.87	1.87	2.96	2.96
k_{1113}		–0.03			0.04		–0.08	
k_{112a2a}	–10.13	–10.13	–10.13	–9.83	–9.83	–9.83	–10.15	–10.15
k_{112b2b}	–10.13	–10.13	–10.13	–9.83	–9.83	–9.83	–10.15	–10.15
k_{1133}	18.97	18.97	18.97	18.97	18.97	18.97	20.10	20.10
k_{12a2a3}		0.03			0.04		0.12	
k_{12b2b3}		0.03			0.04		0.12	
k_{1333}		0.01			0.02		0.03	
$k_{2a2a2a2a}$	2.27	2.27	2.27	2.14	2.14	2.14	2.13	2.13
k_{2a2a33}	–27.57	–27.57	–27.58	–26.02	–26.02	–26.02	–30.40	–30.40
$k_{2b2b2b2b}$	2.27	2.27	2.27	2.14	2.14	2.14	2.13	2.13
k_{2b2b33}	–27.57	–27.57	–27.58	–26.02	–26.02	–26.02	–30.40	–30.40
k_{3333}	6.28	6.28	6.28	5.93	5.93	5.93	7.14	7.14

of the site centre. Its **z**-axis is collinear to the C_2 symmetry axis (direction of the two replaced atoms in the perfect lattice) which corresponds to the equilibrium orientation $\theta^e = \pi/2$ and $\varphi^e = -\pi/4$. The distortion of the argon atoms around the molecule in this site is anisotropic, 4% of the mean site diameter, with a rather cylindrical symmetry. The corresponding minimum energy value $V_M^{(2)e}$ is then –2 100 cm^{-1}.

In the case of N_2O, the total energy of the molecule-matrix system is positive when the molecule is placed in a single substitutional site. In the double substitutional site, as for CO_2, the equilibrium position corresponds to the molecular axis being along the C_2 symmetry axis of this site, with the centre of mass of the molecule at ±0.17 Å from the site centre, and the oxygen atom closest to the argon atom on this axis (see Fig. 1). The distortion that results from the fit of experimental and calculated vibrational fundamental modes is twice as great as that for CO_2 in the S2 site. It is anisotropic, that is, unequal in the two perpendicular planes containing the molecular axis. Finally the minimum energy value $V_M^{(2)e}$ for this molecule is –2 070 cm^{-1}.

3.2 Vibrational frequency shifts

The harmonic and anharmonic vibrational potential constants are computed from gas phase values given by Suzuki for CO_2 [20] and N_2O [21] molecules. Results are given in Table 2. To take into account the lifting of the degeneracy of the ν_2 mode for molecules trapped in sites S2, the constants are given for four vibrational modes labelled $\nu_1, \nu_{2a}, \nu_{2b}$ and ν_3, to make a comparison with gas phase values easier. For molecules trapped in sites S1, the ν_2 mode is degenerate and constants connected to ν_{2b} may be ignored, since they are the same as for ν_{2a}. The results given in Table 2 show that only harmonic and third order constants are changed in the matrix environment, the change being more pronounced for harmonic ones, as was found for the O_3 molecule [2,3]. Moreover, in site S2, new terms, corresponding to a change in the symmetry of the potential in which the nuclei move, are generated by the molecule-matrix interaction. In particular, one may note the third order term k_{113} for CO_2, and fourth order terms such as k_{12a2a3}, k_{12b2b3}, and k_{1333} for both CO_2 and N_2O. Up to second order, the energy levels for non-degenerate

Table 3. Harmonic frequencies and anharmonic constants (cm^{-1}) for $^{12}CO_2$, $^{13}CO_2$ and $^{14}N_2O$ molecules trapped in the S1 and S2 sites of argon matrices and their values in the gas phase [20,21].

	$^{12}CO_2$			$^{13}CO_2$			$^{14}N_2O$	
	S1	S2	gas	S1	S2	gas	S2	gas
ω_1	1361.0	1354.6	1354.0	1360.3	1354.6	1354.0	1298.4	1300.4
ω_{2a}	667.5	669.4	673.2	648.3	650.1	654.0	597.2	596.5
ω_{2b}	667.5	669.0	673.2	648.3	649.7	654.0	596.3	596.5
ω_3	2392.5	2386.5	2396.3	2324.1	2318.0	2328.1	2276.7	2281.6
x_{11}	–3.0	–2.9	–2.9	–3.0	–2.9	–2.9	–5.0	–4.9
x_{12}	–3.6	–3.6	–3.6	–3.5	–3.5	–3.5	–5.0	–5.0
x_{13}	–20.4	–20.3	–19.7	–19.3	–19.2	–19.2	–27.3	–27.4
x_{22}	1.1	1.1	1.1	1.0	1.0	1.0	0.9	0.9
x_{23}	–12.3	–12.4	–12.4	–11.6	–11.6	–11.6	–14.1	–14.1
x_{33}	–12.5	–12.5	–12.5	–11.7	–11.7	–11.7	–15.1	–15.1
$x_{l_2l_2}$	–0.9	–0.9	–0.9	–0.8	–0.8	–0.8	–0.9	–0.9

vibrations can be computed from the formula [1]

$$G(v) = \sum_i \omega_i (v_i + \frac{d_i}{2}) + \sum_{i \le j} x_{ij} (v_i + \frac{d_i}{2})(v_j + \frac{d_j}{2}). \quad (13)$$

where $d_i = d_j = 1$. In the case of linear triatomics with the ν_2 mode doubly degenerate, then $d_2 = 2$ and a third term, $x_{l_2l_2}l^2$ is added to take into account internal rotation with respect to the internuclear axis. We note that if the molecular Hamiltonian is written as $H = H'_0(\text{diagonal}) + H'_2(\text{diagonal}) + H'_1(\text{off-diagonal})$ where H'_1 and H'_2 are third order and fourth order terms appearing in H'_a (Eq. (8)), then the anharmonic constants x_{ij} are given by the matrix elements of H'_a. The latter lead to formulae given in Appendix B [4]. One may note that the fourth order terms such as k_{12a2a3}, k_{12b2b3}, and k_{1333} do not appear in these formulae, because they correspond to third order anharmonic corrections. Such formulae have been directly applied for molecules trapped in sites S1 (degenerate ν_2 mode). For molecules trapped in sites S2, ω_2 is either $\overline{\omega}_2 + \delta$ or $\overline{\omega}_2 - \delta$, where $\overline{\omega}_2 = (\omega_{2a} + \omega_{2b})/2$ and $\delta = (\omega_{2a} - \omega_{2b})/2$ are two parameters that have been defined in reference [1] (Eq. (21)). Let us recall that ω_{2a} and ω_{2b} are then considered as quasi-degenerate modes and in that case the corresponding vibrational energy levels are determined by applying degenerate perturbation theory using a three-dimensional Wang basis (see Eq. (18) of Ref. [1]). The values calculated for the harmonic frequencies ω_i and the anharmonic constants x_{ij} are given in Table 3 and the corresponding vibrational energies for $^{12}CO_2$, $^{13}CO_2$ and $^{14}N_2O$ are given in Tables 4, 5 and 6, respectively. Note that, following Rothman *et al.* [22], we are using HITRAN notation for the labelling of the energy levels. For levels perturbed by Fermi resonance, such as 10^00 and 02^00 for instance, the labelling is 10^00 (1) and 10^00 (2), where number (1) is assigned to the highest of the two levels. Observed and calculated values agree to within experimental accuracy. One may note that while the ω_i values are different for the gas and the matrix perturbed molecule, the x_{ij} are, on the contrary, hardly changed by the effect of the matrix.

3.3 Orientational level schemes

Following the models developed in Section 2.3, the angular potential surfaces $V_M^{(n)}(\mathbf{\Omega})$ experienced by the rigid molecules at their centre of mass equilibrium positions in the distorted (static cage) argon matrix have been expanded up to the sixth power of the new u variables. The expressions obtained show that for CO_2, because of its symmetry, all terms of odd u-powers are zero, while for N_2O these terms do not disappear but remain vanishingly small.

In Table 7 we give the calculated harmonic librational frequencies and the energy values connected to the first fifteen librational states (up to $\sim$200 cm^{-1}) for CO_2 trapped in S1 and S2 sites and N_2O trapped in the S2 site of the argon matrix. The first two columns characterize the level schemes of CO_2 molecules trapped in the S1 sites and connected, respectively, to the one-dimensional librational θ motion around the **Z** absolute axis ($\theta^e = 0$), φ motion being free; and to the two-dimensional librational θ and φ motions around the **X** absolute axis ($\theta^e = \pi/2$, $\varphi^e = 0$) and the **Y**-axis ($\theta^e = \pi/2$, $\varphi^e = \pi/2$). They consist of well separated sets of 1, 2, 3, 4 and 5 levels. The differences which appear between these level schemes are due to the different applied models.

In the double substitutional site, though the sets of levels are separated for the N_2O molecule, they tend to be intermixed for the CO_2 molecule. This can be explained by the sufficiently large difference between the librational frequencies connected to the θ and φ motions for CO_2 than for N_2O.

Finally, at the low temperature range considered (T = 5 K), only the vibration-orientation ground state ($v_k = 0, j_i = 0, m_i = 0$) is populated and thus all transitions start from this state. As a matter of fact, the population of the first excited state ($v_k = 0, j_i = 0, m_i = 1$) connected

Table 4. Calculated and observed vibrational level scheme (cm^{-1}) for a $^{12}CO_2$ molecule trapped in an argon matrix and in the gas phase, up to 2 350 cm^{-1}.

	matrix				gas		
band	site	observed	calculated	obs-calc	observed	calculated	obs-calc
00^01	S1	2344.88	2345.08	–0.20	2349.16	2349.14	+0.02
	S2		2339.05				
11^10 (1)	S1		2071.66		2076.45	2076.75	–0.30
	S2		2072.00				
	S2		2071.16				
03^30 (1)	S1		1986.95		2003.28	2004.08	–0.80
	S2		1992.80				
	S2		1991.57				
11^10 (2)	S1		1921.83		1932.47	1932.90	–0.43
	S2		1922.94				
	S2		1922.13				
10^00 (1)	S1		1387.86		1388.19	1388.08	+0.11
	S2		1385.96				
	S2		1385.56				
02^20 (1)	S1		1324.21		1335.13	1335.61	–0.48
	S2		1328.09				
	S2		1327.27				
10^00 (2)	S1		1281.12		1285.41	1285.65	–0.24
	S2		1280.56				
	S2		1280.14				
01^10	S1	661.96	661.89	+0.07	667.38	667.58	–0.20
	S2	663.82	663.82	0.00			
	S2	663.41	663.41	0.00			

to a CO_2 molecule trapped in the S2 site (see Tab. 7) does not exceed 0.003% of the total population in this site. The canonical partition function is then $Z^{(n)} \simeq 1$ for CO_2 and N_2O.

3.4 Infrared bar spectra

Using equation (12), the integrated absorption coefficients $I_2^{(n)}$ and $I_3^{(n)}$, associated with the ν_2 (bending) and ν_3 (stretching) vibrational modes of CO_2 and N_2O monomers trapped in the n substitutional site of argon matrix, have been calculated (in arbitrary unit and in terms of $\mathcal{N}^{(n)}$, the numbers of monomers per volume unit) at the low temperature $T = 5$ K. The transition elements of the dimensionless vibrational normal coordinates $\langle ...0_k... | q_k | ...1_k... \rangle = 1/\sqrt{2}$ were used, corresponding to the harmonic oscillator approximation. The more intense calculated peaks are connected to the pure vibration transitions $|...0_k...\rangle|00\rangle^{(n)} \rightarrow |...1_k...\rangle|00\rangle^{(n)}$; all other possible vibration-orientation transitions are very weak, their intensities being less than 2% of the more intense line in the ν_k frequency region.

For the N_2O species trapped in an argon matrix, it has been mentioned above that all molecules are trapped in the double substitutional site ($\mathcal{N} = \mathcal{N}^{(2)}$). Then in the ν_3 frequency region, only one peak of intensity $147.5\mathcal{N}^{(2)}$ was obtained at 2 218.9 cm^{-1}. In the ν_2 (doubly degenerate mode) region, two peaks of same intensity $1.4\mathcal{N}^{(2)}$ at frequencies 588.6 and 589.5 cm^{-1} were calculated; they are due to the splitting of the degeneracy of this mode owing to the anisotropy of the trapping site. The intensity ratio $I_3^{(2)}/I_2^{(2)}$ is equal to 52.5.

For the CO_2 species, in the ν_3 frequency region, two intense peaks of intensities $249.2\mathcal{N}^{(1)}$ and $248.5\mathcal{N}^{(2)}$ were obtained at 2 345.1 and 2 339 cm^{-1}, associated with molecules trapped in the single S1 and double S2 substitutional sites, respectively.

In the ν_2 region, three intense peaks were obtained; one of intensity $14.9\mathcal{N}^{(1)}$ at frequency 661.9 cm^{-1}, arising from molecules trapped in the S1 sites, and two of same intensity $11.2\mathcal{N}^{(2)}$ at frequencies 663.4 and 663.8 cm^{-1}, arising from molecules trapped in the S2 sites, at which there occurs a splitting of the mode degeneracy caused by the site anisotropy, as for the N_2O case. The corresponding intensity ratios $I_3^{(1)}/I_2^{(1)}$ and $I_3^{(2)}/I_2^{(2)}$ are equal to 16.7 and 11.1, respectively. We note, however, that these ratios are independent of the numbers $\mathcal{N}^{(1)}$ and $\mathcal{N}^{(2)}$ of monomers in the matrix sites.

Finally, one must note that selection rules show that molecules trapped in the S1 sites and librating around the **Z**-axis of the absolute frame do not participate in

Table 5. Calculated and observed vibrational level scheme (cm^{-1}) for a $^{13}CO_2$ molecule trapped in an argon matrix and in the gas phase, up to 2 285 cm^{-1}.

	matrix				gas		
band	site	observed	calculated	obs-calc	observed	calculated	obs-calc
$00^0 1$	S1	2279.51	2279.48	+0.03	2283.48	2283.50	–0.02
	S2	2273.66	2273.43	+0.23			
$11^1 0$ (1)	S1		2034.82		2037.50	2037.32	+0.18
	S2		2033.98				
	S2		2033.22				
$03^3 0$ (1)	S1		1930.34		1946.40	1946.26	+0.14
	S2		1935.69				
	S2		1934.40				
$11^1 0$ (2)	S1	1882.10	1882.92	–0.82	1896.93	1896.68	+0.25
	S2	1884.41	1885.15	–0.74			
	S2	1884.01	1884.19	–0.18			
$10^0 0$ (1)	S1		1373.02		1370.05	1370.21	–0.16
	S2		1369.81				
	S2		1369.54				
$02^2 0$ (1)	S1	1286.10	1286.50	–0.40	1297.70	1297.76	–0.06
	S2	1288.41	1290.05	–1.64			
	S2	1288.01	1289.19	–1.18			
$10^0 0$ (2)	S1	1257.10	1258.03	–0.93	1265.81	1265.83	–0.02
	S2	1258.41	1259.09	–0.68			
	S2	1258.01	1258.49	–0.48			
$01^1 0$	S1	643.10	643.05	+0.05	648.91	648.67	+0.24
	S2	644.91	644.82	+0.09			
	S2	644.51	644.39	+0.12			

Table 6. Calculated and observed vibrational level scheme (cm^{-1}) for a $^{14}N_2O$ molecule trapped in an argon matrix and in the gas phase, up to 2224 cm^{-1}.

	matrix				gas		
band	site	observed	calculated	obs-calc	observed	calculated	obs-calc
$00^0 1$	S2	2218.60	2218.80	–0.20	2223.76	2223.64	+0.12
$11^1 0$ (1)	S2	1879.30	1879.42	–0.12	1880.27	1880.66	–0.39
	S2	1878.10	1878.44	–0.34			
$03^3 0$ (1)	S2		1771.12		1766.92	1766.46	+0.46
	S2		1769.00				
$11^1 0$ (2)	S2		1750.03		1749.06	1749.16	–0.10
	S2		1748.19				
$10^0 0$ (1)	S2		1283.05		1284.91	1285.14	–0.23
	S2	1282.80	1282.89	–0.09			
$02^2 0$ (1)	S2		1179.90		1177.75	1177.64	+0.11
	S2		1178.49				
$10^0 0$ (2)	S2		1168.53		1168.13	1168.26	–0.13
	S2	1167.60	1167.34	+0.26			
$01^1 0$	S2	589.40	589.53	–0.13	588.77	588.82	–0.05
	S2	588.50	588.82	–0.32			

Table 7. Level schemes connected to the angular motions of the rigid linear CO_2 and N_2O molecules trapped in argon matrices. ω are the harmonic librational frequencies and $\mathcal{E}$ are the energies obtained by introducing the anharmonic remaining terms of the Hamiltonians.

		CO_2		N_2O
trapping site	S1	S1	S2	S2
equilibrium Orientation	$\theta^e = 0$	$\theta^e = \pi/2$	$\theta^e = \pi/2$	$\theta^e = \pi/2$
	φ free	$\varphi^e = 0, \pi/2$	$\varphi^e = -\pi/4$	$\varphi^e = -\pi/4$
ω_θ (cm^{-1})	52.9	49.9	57.4	51.3
ω_φ (cm^{-1})	–	52.6	39.0	43.7
energy level (cm^{-1})	$\mathcal{E}$ (j, M)	$\mathcal{E}$ (j, m)	$\mathcal{E}$ (j, m)	$\mathcal{E}$ (j, m)
	0 (0, 0)	0 (0, 0)	0 (0, 0)	0 (0, 0)
	49.3 (1, +1)	49.9 (1, 0)	36.5 (0, 1)	41.2 (0, 1)
	49.3 (1, –1)	54.5 (0, 1)	53.3 (1, 0)	48.3 (1, 0)
	95.7 (1, 0)	98.3 (2, 0)	72.4 (0, 2)	80.9 (0, 2)
	96.1 (2, +2)	107.2 (1, 1)	86.2 (1, 1)	87.5 (1, 1)
	96.1 (2, –2)	109.2 (0, 2)	104.2 (2, 0)	94.5 (2, 0)
	139.9 (2, +1)	145.3 (3, 0)	107.5 (0, 3)	119.1 (0, 3)
	139.9 (2, –1)	158.7 (2, 1)	118.4 (1, 2)	125.2 (1, 2)
	140.5 (3, +3)	164.5 (0, 3)	133.5 (2, 1)	131.8 (2, 1)
	140.5 (3, –3)	165.1 (1, 2)	152.8 (3, 0)	138.7 (3, 0)
	180.8 (2, 0)	190.8 (4, 0)	141.9 (0, 4)	155.7 (0, 4)
	181.2 (3, +2)	208.6 (3, 1)	150.0 (1, 3)	161.5 (1, 3)
	181.2 (3, –2)	219.4 (2, 2)	162.2 (2, 2)	167.5 (2, 2)
	182.5 (4, +4)	220.0 (0, 4)	178.6 (3, 1)	174.0 (3, 1)
	182.5 (4, –4)	223.2 (1, 3)	199.1 (4, 0)	180.8 (4, 0)

the intensity peak connected to the $|...0_2...\rangle|00\rangle^{(1)} \rightarrow |...1_2...\rangle|00\rangle^{(1)}$ pure vibration transition. This effect arises because the transition elements with $\Delta j = 0, \Delta M = 0$ (see Eqs. (9)) of the angular functions associated with the first derivative components of the molecular dipole moment with respect to the q_2 normal coordinate, are zero in this case. However, those with $\Delta j = 0, \Delta m = 0$ (see Eqs. (10)) connected to molecules librating around **X** or **Y** axes are ~ 1. Thus, statistically only 2/3 of the number of molecules per unit volume trapped in S1 sites contribute to the $14.9\mathcal{N}^{(1)}$ intensity peak of CO_2.

4 Comparison with experiments and discussion

To test the validity of the models developed in the present work, we compare the vibrational frequency shifts and integrated absorption coefficients calculated in the last section with the observed values of these quantities.

Observed frequencies have been recorded either by conventional spectroscopic methods or indirectly using laser induced fluorescence (LIF) [9,23–25]. Our calculated values compare well with the observed ones. We note that, in the case of transitions determined from LIF experiments and relating to excited levels, calculations give 625, 596 and 615 cm^{-1} for transitions actually observed at 626, 595 and 615 cm^{-1} in site S1 and 627, 595 and 614 cm^{-1} for transitions actually observed at 627, 596 and 614 cm^{-1} in site S2 [23]. In a previous theoretical work on the spectroscopy of N_2O trapped in an N_2 matrix, using the method of contact transformation, Smith *et al.* [26] concluded that changes in the vibrational spectrum between the gas phase and the matrix phase could be explained by adjusting only the quadratic force constants, since the changes are insignificant when the cubic and quartic constants are adjusted. The present work shows that such a conclusion is also valid for CO_2 and N_2O trapped in argon, if one calculates vibrational energies up to the second order anharmonic constants x_{ij} (see Tab. 1). However, the changes in the third and fourth order potential constants (see Tab. 2) for molecules trapped in sites S2 should be taken into account if third order anharmonic constants (higher than x_{ij}) are considered in vibrational energy calculations. For low-lying levels up to 2 800 cm^{-1} they can be neglected.

As far as the matrix effects are concerned (Eq. (6)), they have been determined up to the second order *via* β_i and β_{ij}, the first and second derivatives of $V_M^{(n)}(\{q\})$ with respect to the dimensionless normal coordinates q. As already pointed out in Section 2.2, two different electric fields, a static one and a dynamic one, contribute to the latter parameters. In the case of N_2O, the present work shows that, using the fixed gas phase values for the molecular dipole and quadrupole moments, the effects of matrix distortion and polarization around the trapped molecule account for the shifts of the three fundamental vibrational modes ν_1, ν_2 and ν_3. For CO_2, the same is true for the

Table 8. Characteristics of the experimental spectra of CO_2 and N_2O molecules trapped in argon matrices from references [1, 24,25]. ω_k (cm^{-1}) are the frequency positions of the line intensity maxima I_k^{max} (arbitrary units), γ_k (cm^{-1}) their full widths at half maxima (FWHM), while I_3/I_2 is the integrated intensity ratio.

	CO_2			N_2O	
trapping site	S1	S2		S2	
ν_2 mode					
ω_2	661.9	663.4	663.8	588.5	589.4
γ_2	0.09	0.035	0.035	0.075	0.09
I_2^{max}	0.23	0.14	0.12	0.62	0.74
ν_3 mode					
ω_3	2345.1	2339.0		2218.6	
γ_3	0.36	0.12		0.14	
I_3^{max}	0.81	0.75		4.95	
I_3/I_2	12.7	5.7		48.3	

modes ν_1 and ν_3. We note that for mode ν_1, we are referring to the levels 10^00 (1) and 10^00 (2) since mode ν_1 is not observed, being IR inactive. In reference [1] the shifts calculated for the ν_2 mode are less than the observed shifts by a factor slightly greater than 2 for both trapping sites. In the model, the experimental shift is achieved by increasing the effect of the dynamic electric field, that is by increasing $b_M^{\nu_2}$, the first derivative of the dipole moment (see Appendix A) with respect to the normal coordinate q_2, by a factor of 1.7 in the S1 site and of 2 in the S2 site. As a matter of fact, high resolution experimental infrared spectra in the ν_2 and ν_3 vibrational frequency regions of CO_2 and N_2O species trapped in argon matrices at low temperature have been reported [1,24,25]. The characteristic quantities for the lines attributed to monomers are summarized in Table 8. For the N_2O species, the authors [24, 25] measured an integrated intensity ratio $I_3/I_2 = 48.3$, consistent with the gas phase value, while for the CO_2 species the measured ratios were 12.7 in the S1 trapping sites and 5.7 in the S2 sites. We note that in the case of CO_2, if the experimental determination is correct, then the increase in $b_M^{\nu_2}$, the first derivative of the dipole moment of CO_2 with respect to the normal coordinate q_2, seems to be corroborated both by experiment and calculation.

This surprising ratio difference for the CO_2 species was explained by the authors [24,25] in terms of the distribution of monomers in the two matrix sites: (i) in the ν_2 frequency region, about 52% of the intensity is due to monomers trapped in S1 sites and $\sim$ 48% is due to monomers trapped in S2 sites, and (ii) in the ν_3 region, the corresponding values are $\sim$ 72% and $\sim$ 28%, respectively.

Comparison between measured and calculated intensity ratios $I_3^{(n)}/I_2^{(n)}$ shows a good agreement for the N_2O species but a poorer one for CO_2. Indeed, such a comparison does not allow determination of the distribution of CO_2 monomers in the two sites. Accordingly, we propose a comparison in terms of the ratios $I_k^{max(1)}/I_k^{max(2)}$ of the band intensity maxima in the ν_2 region, on the one hand, and in the ν_3 region, on the other hand.

To carry out such a comparison, we consider a Lorentzian model for the lines and use the experimental linewidths to determine their intensity maxima $I_k^{max(n)} = 2I_k^{(n)}/\gamma_k^{(n)}$ for each site n. The ratios $I_k^{max(1)}/I_k^{max(2)}$ are then calculated and adjusted to the corresponding experimental ones. The obtained distributions are as follows:

(i) $\mathcal{N}^{(1)} = 77\%\mathcal{N}$, $\mathcal{N}^{(2)} = 23\%\mathcal{N}$ in the ν_2 region;
(ii) $\mathcal{N}^{(1)} = 76\%\mathcal{N}$, $\mathcal{N}^{(2)} = 24\%\mathcal{N}$ in the ν_3 region.

Considering the uncertainties of the latter model, one can see that these distributions are identical and clearly agree with the experimental distribution ($\sim$ 72% and $\sim$ 28% mentioned above) given for the ν_3 region [24]. Note however that the difference between calculated and experimental distributions in the ν_2 region is only an apparent one. In effect, as has been mentioned above, only 2/3 of the $\mathcal{N}^{(1)}$ molecules in the S1 sites contribute to the line intensity in this region. Thus the intensities due to molecules trapped in S1 and S2 sites are $\sim$ 51% and $\sim$ 49%, respectively, which agree with the experimental values ($\sim$ 52% and $\sim$ 48%) mentioned above [24].

Finally, we note that the agreement between the calculated bar-spectra and the experimental spectra clearly shows the pertinence of the calculations and the renormalization procedure developed in this theoretical approach. However, such a model is too crude to account fully for the experimental conditions; our calculations were made for ideal molecule-matrix systems. The calculated shape of the bar-spectrum is generally very sensitive to the degree of knowledge of the molecular motions; this itself strongly depends on the accuracy of both the potential energy model used to describe the interaction between the molecule and the surrounding matrix and of the convergence of the expansion of this potential in terms of the relevant coordinates.

Moreover, in the orientational level schemes given in Table 7, additional level shifts can occur depending on the v_k vibrational state of the molecules. As a matter of fact, the potential energy surfaces $V_M^{(n)}(\mathbf{\Omega})$ and the rotational constants B of the molecules depend parametrically on the vibrational state and therefore equations (9, 10) must

be solved for both the fundamental $v_k = 0$ and first excited $v_k = 1$ states. As a consequence, the line frequency positions in the bar-spectra should be slightly shifted.

Finally, as far as orientational levels are concerned, the fact that they are differently arranged for N_2O and CO_2 in the S2 site, being more dense for the latter, may explain the results of laser induced fluorescence (LIF) experiments on both molecules. At a dilution of 1/2000, 10 μm fluorescence ($00^01 \rightarrow 10^00$ (1)) is observed when the ν_3 mode is pumped for N_2O, whereas with CO_2 only 16 μm fluorescence (11^10 (2) $\rightarrow 02^20$ (1), 11^10 (2) $\rightarrow 10^00$ (2) and 10^00 (2) $\rightarrow 01^10$ (1)) is observed [24,25]. The close spacing of orientational levels for CO_2 decreases the lifetime of the pumped ν_3 level and relaxation is mainly non-radiative for dilute samples. In the case of N_2O, the lifetime of the pumped level is such that radiative relaxation through 10 μm is possible.

5 Conclusion

In conclusion we note that the theoretical model developed in this work allows computation of low-lying vibrational energy levels from a fit of the experimental and calculated frequencies of fundamental modes. For such levels, shifts are mainly due to changes in the harmonic potential constants only, although matrix third and fourth order potential constants show a change in the symmetry of the potential in which the nuclei vibrate. In the case of CO_2, the matrix dipole moment associated with the ν_2 mode seems to be greater than that of its gas phase value. As far as trapping sites are concerned, the model shows unambiguously that N_2O is trapped in a double site, resulting in a lifting of the degeneracy of the ν_2 vibrational mode, as suggested by Sodeau *et al.* [6]. Moreover, the bar-spectra calculated using our model of the orientational motions of the trapped molecules are in good agreement with the experimental spectra. In particular, for the ν_2 mode of CO_2, the resulting experimental distribution of monomers trapped in the S1 (52%) and S2 (48%) sites is interpreted using the fact that only 2/3 of the CO_2 monomers in the S1 site contribute to the line intensity.

As far as the orientational level schemes are concerned for CO_2 and N_2O in the S2 site, our results are consistent with LIF experimental observations.

Helpful assistance of F. Gazelle and B. Debray (Observatoire de Besançon) are gratefully acknowledged. We are also grateful to Prof. J. Killingbeck and the referees for fruitful comments.

Appendix A: Rotational matrix transformation and molecular dipole moment

The unitary matrix $\mathbf{M}$ characterizing the transformation from the crystal absolute frame (**X, Y, Z**) to the frame (**x, y, z**) associated with the linear molecule through the Euler angles (φ, θ) is given as [27]

$$\mathbf{M}(\varphi,\theta) = \begin{pmatrix} \cos\varphi\cos\theta & \sin\varphi\cos\theta & -\sin\theta \\ -\sin\varphi & \cos\varphi & 0 \\ \cos\varphi\sin\theta & \sin\varphi\sin\theta & \cos\theta \end{pmatrix}. \quad (A.1)$$

In order to calculate the infrared absorption coefficient, the molecular dipole moment $\boldsymbol{\mu}_{\mathrm{M}}$, in the frame (**x, y, z**), is expanded, up to the first order, in terms of the dimensionless vibrational normal coordinates q as

$$\boldsymbol{\mu}_{\mathrm{M}} = \boldsymbol{\mu}^{\mathrm{e}}_{\mathrm{M}} + \sum_k \mathbf{b}^{\nu_k}_{\mathrm{M}} q_k, \quad (A.2)$$

where $\boldsymbol{\mu}^{\mathrm{e}}_{\mathrm{M}}$ is the permanent dipole moment and $\mathbf{b}^{\nu_k}_{\mathrm{M}}$ the first derivative of $\boldsymbol{\mu}_{\mathrm{M}}$ with respect to the kth normal coordinate q_k. Thus, in the absolute frame, the molecular dipole moment $\boldsymbol{\mu}_A$ and its first derivative $\partial\boldsymbol{\mu}_A/\partial q_k$ can be written as

$$\begin{aligned} \boldsymbol{\mu}_A &= \mathbf{M}^{-1}(\varphi,\theta)\boldsymbol{\mu}_M, \\ \frac{\partial\boldsymbol{\mu}_A}{\partial q_k} &= \mathbf{M}^{-1}(\varphi,\theta)\mathbf{b}^{\nu_k}_M, \end{aligned} \quad (A.3)$$

in which $\mathbf{M}^{-1}$ is the inverse matrix of $\mathbf{M}$ defined above. Thus the first derivatives of the molecular dipole moment with respect to each normal coordinate are given by

$$\begin{aligned} \frac{\partial\boldsymbol{\mu}_A}{\partial q_1} &= \mathrm{b}^{\nu_1}_{\mathrm{M}}\left(\cos\varphi\sin\theta\mathbf{X} + \sin\varphi\sin\theta\mathbf{Y} + \cos\theta\mathbf{Z}\right), \\ \frac{\partial\boldsymbol{\mu}_A}{\partial q_{2a}} &= \mathrm{b}^{\nu_{2a}}_{\mathrm{M}}\left(\cos\varphi\cos\theta\mathbf{X} + \sin\varphi\cos\theta\mathbf{Y} - \sin\theta\mathbf{Z}\right), \\ \frac{\partial\boldsymbol{\mu}_A}{\partial q_{2b}} &= \mathrm{b}^{\nu_{2b}}_{\mathrm{M}}\left(-\sin\varphi\mathbf{X} + \cos\varphi\mathbf{Y}\right), \\ \frac{\partial\boldsymbol{\mu}_A}{\partial q_3} &= \mathrm{b}^{\nu_3}_{\mathrm{M}}\left(\cos\varphi\sin\theta\mathbf{X} + \sin\varphi\sin\theta\mathbf{Y} + \cos\theta\mathbf{Z}\right). \end{aligned} \quad (A.4)$$

The $b^{\nu_k}_{\mathrm{M}}$ values are given in Table 9 for CO_2 and N_2O molecules and the orientational functions must be developed in terms of the variables defined in equations (9, 10) in order to calculate the orientational transition elements.

Table 9. First derivative values $b^{\nu_k}_{\mathrm{M}}$ (Debye) of the molecular dipole moment with respect to the dimensionless normal coordinates q_k for CO_2 and N_2O in the gas phase.

	CO_2	N_2O
$b^{\nu_1}_{\mathrm{M}}$	0.0	0.1921
$b^{\nu_{2a}}_{\mathrm{M}}$	–0.1839	–0.0685
$b^{\nu_{2b}}_{\mathrm{M}}$	–0.1839	–0.0685
$b^{\nu_3}_{\mathrm{M}}$	0.4610	–0.3647

Appendix B: Anharmonic vibrational constants and Fermi-Dennisson resonance for linear triatomic molecules

B.1 Anharmonic vibrational constants

The expressions of the anharmonic vibrational constants for linear triatomic molecules are

$$x_{ss} = \frac{1}{4}\left\{6k_{ssss} - \frac{15k_{sss}^2}{\omega_s} - \frac{k_{sss'}^2}{\omega_{s'}}\left(\frac{8\omega_s^2 - 3\omega_{s'}^2}{4\omega_s^2 - \omega_{s'}^2}\right)\right\}, \quad (s = 1,3; s' = 3,1);$$

$$x_{22} = \frac{1}{4}\left\{6k_{2222} - \frac{k_{122}^2}{\omega_1}\left(\frac{8\omega_2^2 - 3\omega_1^2}{4\omega_2^2 - \omega_1^2}\right) - \frac{k_{223}^2}{\omega_3}\left(\frac{8\omega_2^2 - 3\omega_3^2}{4\omega_2^2 - \omega_3^2}\right)\right\};$$

$$x_{2s} = \frac{1}{2}\left\{k_{22ss} - \frac{4k_{22s}^2\omega_2}{(4\omega_2^2 - \omega_s^2)} - \frac{k_{22s'}k_{s'ss}}{\omega_{s'}} + 2\frac{\omega_s}{\omega_2}\left(\zeta_{2s}^{(z)}\right)^2 B_e\right\}, (s = 1,3; s' = 3,1);$$

$$x_{s2} = \frac{1}{2}\left\{k_{ss22} - \frac{6k_{sss}k_{s22}}{\omega_s} - \frac{k_{sss'}k_{s'22}}{\omega_{s'}} + 2\frac{\omega_2}{\omega_s}\left(\zeta_{s2}^{(z)}\right)^2 B_e\right\}, (s = 1,3; s' = 3,1);$$

$$x_{ss'} = \frac{1}{2}\left\{k_{sss's'} - \frac{6k_{sss}k_{ss's'}}{\omega_s} - \frac{4k_{sss'}^2\omega_s}{(4\omega_s^2 - \omega_{s'}^2)}\right\}, \quad (s = 1,3; s' = 3,1)$$

$$x_{l_2l_2} = -\frac{1}{2}k_{2222} - \frac{k_{221}^2\omega_1}{4(4\omega_2^2 - \omega_1^2)} - \frac{k_{223}^2\omega_3}{4(4\omega_2^2 - \omega_3^2)}.$$

For the N_2O molecule

$$x_{11} = \frac{1}{4}\left\{6k_{1111} - \frac{15k_{111}^2}{\omega_1} - \frac{k_{113}^2}{\omega_3}\left(\frac{8\omega_1^2 - 3\omega_3^2}{4\omega_1^2 - \omega_3^2}\right)\right\};$$

$$x_{33} = \frac{1}{4}\left\{6k_{3333} - \frac{15k_{333}^2}{\omega_3} - \frac{k_{133}^2}{\omega_1}\left(\frac{8\omega_3^2 - 3\omega_1^2}{4\omega_3^2 - \omega_1^2}\right)\right\};$$

$$x_{22} = \frac{1}{4}\left\{6k_{2222} - k_{122}^2\left(\frac{2}{\omega_1} + \frac{1}{2(2\omega_2 + \omega_1)}\right) - \frac{k_{223}^2}{\omega_3}\left(\frac{8\omega_2^2 - 3\omega_3^2}{4\omega_2^2 - \omega_3^2}\right)\right\};$$

$$x_{12} = k_{1122} - \frac{k_{122}^2}{2(2\omega_2 + \omega_1)} - \frac{3k_{111}k_{122}}{\omega_1} - \frac{k_{223}k_{113}}{\omega_3} + \left(\frac{\omega_1^2 + \omega_2^2}{\omega_1\omega_2}\right)(\zeta_{21})^2 B_e;$$

$$x_{23} = k_{2233} - \frac{2k_{223}^2\omega_2}{(4\omega_2^2 - \omega_3^2)} - \frac{3k_{333}k_{223}}{\omega_3} - \frac{k_{122}k_{133}}{\omega_1} + \left(\frac{\omega_2^2 + \omega_3^2}{\omega_2\omega_3}\right)(\zeta_{23})^2 B_e;$$

$$x_{13} = k_{1133} - \frac{2k_{133}^2\omega_3}{(4\omega_3^2 - \omega_1^2)} - \frac{2k_{113}^2\omega_1}{(4\omega_1^2 - \omega_3^2)} - \frac{3k_{111}k_{133}}{\omega_1} - \frac{3k_{333}k_{113}}{\omega_3};$$

$$x_{l_2l_2} = -\frac{1}{2}k_{2222} + \frac{k_{122}^2}{8(2\omega_2 + \omega_1)} - \frac{k_{223}^2\omega_3}{4(4\omega_2^2 - \omega_3^2)},$$

and for the CO_2 molecule

$$x_{11} = \frac{1}{4}\left\{6k_{1111} - \frac{15k_{111}^2}{\omega_1}\right\};$$

$$x_{33} = \frac{1}{4}\left\{6k_{3333} - \frac{k_{133}^2}{\omega_1}\left(\frac{8\omega_3^2 - 3\omega_1^2}{4\omega_3^2 - \omega_1^2}\right)\right\};$$

$$x_{22} = \frac{1}{4}\left\{6k_{2222} - k_{122}^2\left(\frac{2}{\omega_1} + \frac{1}{2(2\omega_2 + \omega_1)}\right)\right\};$$

$$x_{12} = k_{1122} - \frac{k_{122}^2}{2(2\omega_2 + \omega_1)} - \frac{3k_{111}k_{122}}{\omega_1};$$

$$x_{23} = k_{2233} - \frac{k_{122}k_{133}}{\omega_1} + \left(\frac{\omega_2^2 + \omega_3^2}{\omega_2\omega_3}\right)(\zeta_{23})^2 B_e;$$

$$x_{13} = k_{1133} - \frac{2k_{133}^2\omega_3}{(4\omega_3^2 - \omega_1^2)} - \frac{3k_{111}k_{133}}{\omega_1};$$

$$x_{l_2l_2} = -\frac{1}{2}k_{2222} + \frac{k_{122}^2}{8(2\omega_2 + \omega_1)}.$$

B.2 Fermi-Dennisson resonance

The corrective Fermi-Dennisson Hamiltonian element corresponding to the $|v_1, v_2, v_3\rangle \longleftrightarrow |v_1 - 1, v_2 + 2, v_3\rangle$ transition for $(2\omega_2 \cong \omega_1)$, is given by

$$\langle v_1, v_2, v_3|h_{vv'}^{FD}|v_1 - 1, v_2 + 2, v_3\rangle = \frac{k_{122}}{2}\left[\frac{v_1}{2}((v_2 + 2)^2 - l_2^2)\right]^{\frac{1}{2}}.$$

References

1. P.R. Dahoo, I. Berrodier, V. Raducu, J.L. Teffo, H. Chabbi, A. Lakhlifi, L. Abouaf-Marguin, Eur. Phys. J. D **5**, 71 (1999).
2. P.R. Dahoo, A. Lakhlifi, H. Chabbi, J. Chem. Phys. **111**, 10192 (1999).
3. H. Chabbi, P.R. Dahoo, A. Lakhlifi, J. Chem. Phys. **111**, 10202 (1999).
4. H.H. Nielsen, Rev. Mod. Phys. **23**, 90 (1951).
5. J.M. Flaud, C. Camy-Peyret, C.P. Rinsland, M.A.H. Smith, V. Malathy-Devi, *Atlas of Ozone Parameters from Microwave to Medium Infrared* (Academic Press, New York, 1990).
6. J.R. Sodeau, R. Withnall, J. Phys. Chem. **89**, 4484 (1985).
7. L.M. Nuxumalo, T.A. Ford, J. Mol. Struct. **327**, 145 (1994).
8. W.G. Lawrence, V.A. Apkarian, J. Chem. Phys. **97**, 2224 (1992).
9. H. Chabbi, P.R. Dahoo, H. Dubost, A.-M. Vasserot, B. Gauthier-Roy, L. Abouaf-Marguin, Vibrational stimulated emission of CO_2 in inert matrices, *International Conference on Chemistry and Physics in Matrices*, Austria, August 1997.
10. H. Chabbi, I. Berrodier, P.R. Dahoo, J.L. Teffo, A. Lakhlifi, V. Raducu, L. Abouaf-Marguin, Modèle théorique pour le calcul des niveaux d'énergie de molécules piégées en matrice, *J.S.M. III/DIAM V*, Reims, France, July 1998.
11. G. Amat, H.H. Nielsen, J. Chem. Phys. **27**, 845 (1957).
12. G. Amat, H.H. Nielsen, G. Tarrago, *Rotation-Vibration of Polyatomic Molecules* (M. Dekker Inc., New York, 1971).
13. S.H. Lin, J. Chem. Phys. **65**, 1053 (1976).
14. P.A. Flinn, A.A. Maradudin, Ann. Phys. (NY) **18**, 81 (1962).
15. S.C. Wang, Phys. Rev. **34**, 243 (1929).
16. L. Andrews, R.C. Spiker, J. Phys. Chem. **76**, 3218 (1972).
17. M. Spoliti, S.N. Cesaro, B. Mariti, J. Chem. Phys. **59**, 985 (1973).
18. L. Schriver-Mazzuoli, A. Schriver, C. Lugez, A. Perrin, C. Camy-Peyret, J.M. Flaud, J. Mol. Spectrosc. **176**, 85 (1996).
19. I.G. Kaplan, Theory of Molecular Interactions, in *Studies in Physical and Theoretical Chemistry* (Elsevier Scientific Pub. Comp., 1986).
20. I. Suzuki, J. Mol. Spectrosc. **25**, 479 (1968).
21. I. Suzuki, J. Mol. Spectrosc. **32**, 54 (1969).
22. L.S. Rothman, R.L. Hawkins, R.B. Wattson, R.R. Gamache, J. Quant. Spectr. Radiat. Trans. **48**, 537 (1992).
23. H. Chabbi, P.R. Dahoo, B. Gauthier-Roy, A.-M. Vasserot, L. Abouaf-Marguin, M. Broquier, H. Dubost, R. Kolos, A. Tramer, J.M. Berset, J.M. Ortega, Chem. Phys. Lett. **285**, 252 (1998).
24. H. Chabbi, P.R. Dahoo, B. Gauthier-Roy, A.-M. Vasserot, L. Abouaf-Marguin, J. Phys. Chem. A **104**, 1670 (2000).
25. H. Chabbi, P.R. Dahoo, H. Dubost, B. Gauthier-Roy, A.-M. Vasserot, L. Abouaf-Marguin, Low Temp. Phys. (submitted, 2000).
26. D.F. Smith Jr, J. Overend, R.C. Spiker, L. Andrews, Spectrochem. Acta **28**, 87 (1972).
27. M.E. Rose, *Elementary Theory of Angular Momentum* (Wiley, New York, 1967).
28. A. Lakhlifi, C. Girardet, J. Mol. Struct. **110**, 73 (1984).
29. M.L. Klein, J.A. Venables, *Rare Gas Solids.* (Academic Press, London, 1976), Vol. I.
30. D.E. Stogryn, A.P. Stogryn, Mol. Phys. **11**, 371 (1966).